Combination of SEC-MALS and Fluorescence with Molecular Dynamics Simulations for the Analysis of Ionomer Dimensions in Solution. Application to Poly(2-acrylamido-2-methyl-1-propanesulfonic acid-*co*-styrene)

Gema Marcelo, Francisco Mendicuti, Enrique Saiz,* and M. Pilar Tarazona

Departamento de Química Física, Universidad de Alcalá, 28871 Alcalá de Henares, Madrid, Spain

Received October 17, 2006; Revised Manuscript Received December 12, 2006

ABSTRACT: Solution properties of an ionomer, poly(2-acrylamido-2-methyl-1-propanesulfonic acid-*co*-styrene) (PAMPST) with a 95 mol % styrene content, are investigated by using size exclusion chromatography (SEC) coupled with differential refractive index (RI) and multiangle light scattering (MALS) detectors and steady-state fluorescence measurements. Dimensions of ionomers in solution depend on the polarity of the solvent that modifies the interactions of the ionic groups. Measurements were performed in two solvents of very different dielectric constant, namely tetrahydrofuran (THF) and dimethylformamide (DMF), and the addition of a low molecular weight electrolyte such as LiCl to both solvents clearly improves the results affording scaling laws and unperturbed dimensions. In spite of the different thermodynamic quality of the solvents DMF and THF solutions, the extrapolations to unperturbed dimensions provide similar values of the characteristic ratio $C_n = 11-12$. However excimer-to-monomer emission intensity ratios, as consequence of the different origin of excimers, substantially depend on the solvent THF/DMF composition. Molecular dynamics simulations performed on oligomers of PAMPST in THF, THF + LiCl, DMF, and DMF + LiCl solvents support the conclusions obtained from experimental measurements.

1. Introduction

The use of size exclusion chromatography (SEC) with a mass sensitive detector, such as viscosity or light scattering, has become a habitual way of polymer characterization.[1] The combination of a concentration-based detector, such as the usual refractive index (RI) detector, with a multiangle laser light scattering (MALS) detector is particularly advantageous since it offers the possibility of obtaining both molecular weight and dimensions along the chromatogram.[2,3] The dimensions are determined through the root-mean-square radius of gyration, which is a very convenient magnitude to express the size of the chain since its definition is applicable to macromolecules of any shape, and moreover, it can be related to the molecular weight by the scaling relationships.[4,5]

For polymer samples with broad polydispersity, SEC-MALS affords a direct way to measure dimensions vs molecular weight and extrapolate to unperturbed conditions.[6,7] The characterization of polyelectrolytes in aqueous solvents is complicated by the interactions between the electrical charges along the chain that have a strong effect on the dimensions of the chain. Moreover, the addition of salts to the water used in chromatography modifies the electrical interactions and thus the size of the polymer and the elution volume. In spite of these difficulties, the SEC-MALS technique can provide information about polyelectrolytes and thus a better understanding of their solution properties.[8,9]

When a relatively small number of ionic groups (about 15 mol % or less) are added to a nonpolar backbone chain, the resulting ionomers can be dissolved in organic solvents of different polarity. These polymers present polyelectrolyte behavior in polar solvents, whereas the ionic groups associate due to dipolar attractions in low or nonpolar solvents.[10−12] While the application of SEC and light scattering to polyelectrolytes in aqueous solution is relatively widespread, the study of ionomers in organic eluents by these techniques is not as extensive.[11]

The aim of this work is to probe the efficiency of the SEC-MALS technique to the study of ionomers through the scaling laws, unperturbed dimensions, and characteristic ratios. Two solvents of quite different polarity, THF and DMF, both pure and with different amounts of inorganic salts, are used as eluents, and the influence of the presence of salt on the resulting chromatograms is investigated. The addition of small amounts of an electrolyte to an organic solvent such as THF has been used to improve the chromatograms of some neutral polymers such as poly(phosphazenes).[13,14] We have chosen a copolymer of 2-acrylamido-2-methyl-1-propanesulfonic acid and styrene with a styrene content of 95 mol %; i.e., on average, it contains one amide unit separated by 20 styrene residues, as is schematically represented in Figure 1. This polymer, poly(2-acrylamido-2-methyl-1-propanesulfonic acid-*co*-styrene) (PAMPST), is soluble in several organic solvents, and its solution behavior has been studied by viscometry.[15] Thus, our SEC-MALS results can be compared with those previously obtained by a different method. Since most of the repeat units of this polymer contain benzene chromophore groups, fluorescence emission spectra may also give additional information on the variation of the dimensions and polymer interactions upon changing solvent.[16,17] Finally, molecular dynamics simulations performed on systems containing oligomers of PAMPST together with either DMF or THF solvents, both in presence and in absence of ionic salts, allow the evaluation of correlations among rotational angles over the chain backbone and among distances between different groups that can be used to rationalize the experimental results.

* Corresponding author: Tel +34918854664; Fax +34918854763; e-mail enrique.saiz@uah.es.

10.1021/ma0623845 CCC: $37.00
Published on Web 01/19/2007

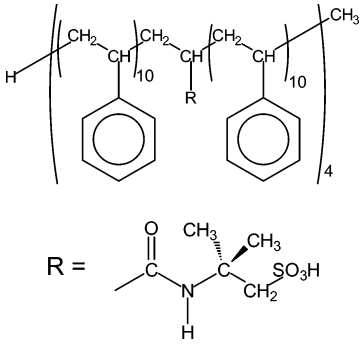

Figure 1. Schematical representation of the PAMPST chain (5% mole content of AM units) as a set of PS segments with average polymerization degree $x = 20$ separated by an AM unit. The oligomer represented in this figure contains 84 repeat units and was employed in all MD simulations (see below).

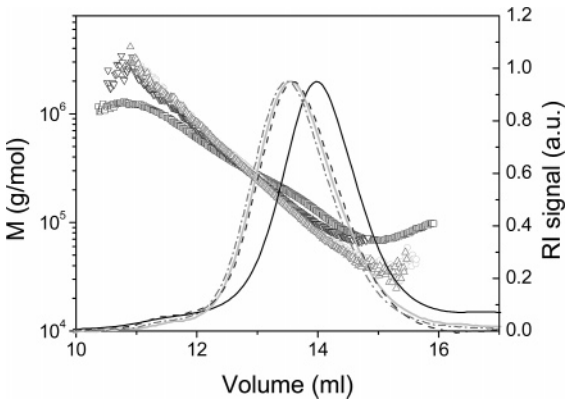

Figure 2. Molecular weight vs elution volume for PAMPST in different organic solutions: THF (square), THF/LiCl 0.05 M (circle), THF/LiCl 0.1 M (triangle), THF/saturated NaCl solution (inverted triangle). Also depicted are the refractive index, RI, signals vs elution volume for PAMPST in THF as solid black line, THF/LiCl 0.05 M as solid light gray line, THF/LiCl 0.1 M as dash-dot gray line, and THF/$NaCl_{sat}$ as a dash dark gray line.

2. Experimental Section

2.1. Materials. Poly(2-acrylamido-2-methyl-1-propanesulfonic acid-*co*-styrene) (PAMPST) was a commercial heterotactic (i.e., fraction of meso diads $w_m \approx 0.4-0.5$) sample (Aldrich). The molar content of styrene was determined by NMR and found to be 95%. Tetrahydrofuran (THF) and dimethylformamide (DMF), GPC grade, lithium chloride, and sodium chloride were obtained from Scharlau. THF, DMF, and several salt solutions (i.e., THF-saturated solution of NaCl, THF solutions 0.05, 0.1, and 0.02 M of LiCl, DMF solution 0.02 M of LiCl) were used as eluents in SEC. All the solvents and solutions used as eluents were filtered through a 0.2 μm PTFE (Millipore) and degassed. They also were checked by fluorescence before using. Polystyrene ($M_w = 95\,800$, Aldrich) and ethylbenzene (Aldrich) were used for some fluorescence measurements.

2.2. Measurements. 2.2.1. SEC-MALS. SEC measurements were carried out using equipment consisted of a Waters Associates model 510 pump with a 0.1 μm on-line filter (Millipore), a U6K injector (Waters), and two different detectors, namely an Optilab interferometric refractometer (RI) operating at 632.8 nm and a Dawn DSP-F multiangle light scattering (MALS) photometer, equipped with a He−Ne laser ($\lambda = 632.8$ nm), both from Wyatt Technology Corp. The eluents used were THF, saturated solution of NaCl, LiCl (0.05 and 0.1 M) in THF, and DMF. The chromatographic columns used, two Styragel linear 10 μm (Waters), for all the eluents were kept in an oven at 25 °C. The use of a third column was investigated, but it did not improve the results. The flow rate was 1 mL/min in the case of THF and 0.3 mL/min for DMF. Repeated injections were made for each sample at different concentrations (<8 mg/mL) to ensure the reproducibility of the results.

The MALS photometer was calibrated with spectrometric grade toluene (Scharlau). The normalization of the detectors in the different organic solutions was performed with low molecular weight standard samples of polystyrene. The software used, ASTRA 4.73 from Wyatt Technology, allowed on-line collection of data of molecular mass and radius of gyration as well as calculation of the distributions and averages.

The values of differential refractive index increment, dn/dc, used were those of polystyrene, namely 0.19 and 0.165 in THF and DMF, respectively, and we used one of the options of the Astra software to verify the suitability of those values from data of injected mass and calibration constant of the interferometric refractometer.[18]

The basic light scattering equation for SEC-MALS[2,19] is

$$\frac{Kc}{\Delta R_\theta} = \left[1 + \frac{16\pi^2}{3\lambda^2}\sin^2\left(\frac{\theta}{2}\right)\langle s^2\rangle_z - ...\right]\left[\frac{1}{M_w}\right] \quad (1)$$

where ΔR_θ is the excess Rayleigh ratio, c is the concentration, λ is the wavelength of the incident light in the medium, θ is the scattering angle, and K is the optical constant given by

$$K = \frac{4\pi^2 n_1^2}{\lambda_0^4 N_A}\left(\frac{dn}{dc}\right)^2 \quad (2)$$

where λ_0 is the vacuum wavelength, n_1 is the solvent refractive index, N_A is Avogadro's number, and dn/dc is the refractive index increment.

The RI detector measures the concentration c of the polymer, and the MALS detector measures simultaneously the excess Rayleigh ratio at different θ angles for each slice i of the chromatogram. Hence, a plot of $Kc/\Delta R_\theta$ vs $\sin^2(\theta/2)$ affords to calculate the molecular mass M_i and the mean-square radius of gyration $\langle s^2\rangle_i$ for each slice across the chromatogram of a polydisperse sample. Consequently, the SEC-MALS results allow the analysis of the variation of the radius of gyration with molecular weight, which is customarily written as a scaling law:

$$\langle s^2\rangle^{1/2} = QM^q \quad (3)$$

where the q coefficient is a universal parameter that provides valuable information about the thermodynamical quality of the solvent and about the size and shape of the polymer.[5,14]

2.2.2. Fluorescence: Instrumentation and Methods. Steady-state fluorescence measurements were performed on an SLM 8100 Aminco spectrofluorimeter equipped with a Xe lamp, a double (single) concave grating monochromator at the excitation (emission) path, and Glan-Thompson prism polarizers in both paths. The photomultiplier was cooled by a Peltier system. The excitation and emission slit widths were set to 16 nm. Right angle geometry, magic angle, and rectangular 10 mm path cells were used for all fluorescence dilute solution measurements. The cell housing temperature (25 °C) was controlled by using a thermostatic bath (Huber Ministat) and measured employing a Pt-100 probe with digital temperature processor (Nokeval model 2011). Solvent baselines were measured and subtracted from the spectra.

3. Results and Discussion

3.1. Chromatograms. Figures 2 and 3 show the RI signal and one of the MALS signals (at 90°), respectively, for PAMPST in the different THF solutions used as eluents. The most significant feature is that the peak for PAMPST in THF is noticeably displaced toward higher elution volumes than those obtained in the same solvent when salts are added. The light scattering signals are proportional to the product of molecular weight and concentration, so they have a different shape than the RI signals that are proportional to concentration. Thus, the small shoulder that appears at low elution volume can be observed more easily in the light scattering signals. The chromatograms obtained when the different salts are added are

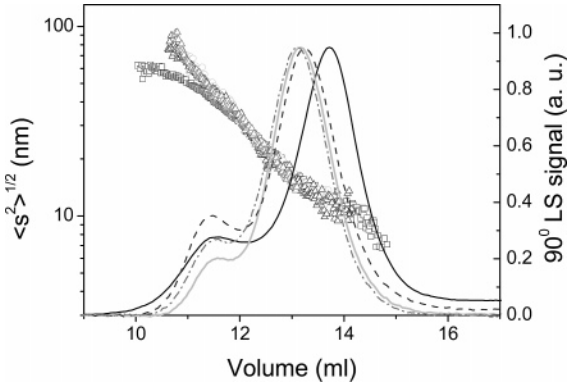

Figure 3. Radius of gyration and 90° MALS signal vs elution volume for PAMPST in the different solvents used. See legend for Figure 2.

very similar. The nature of the cation (i.e., sodium or lithium) produces no significant difference while their concentration seems to slightly modify the shoulder at low elution volumes. This shoulder diminishes when the amount of salt added to the eluent is increased from NaCl, which is scarcely soluble in THF until the LiCl 0.1 M solution. The results obtained when LiCl 0.2 M is used as eluent are similar to those obtained with LiCl 0.1 M and are not depicted in Figures 2 and 3.

The appearance of the chromatograms gives a first insight into the solution behavior of the ionomer and the effect produced by the presence of salt in the eluent. More information can be obtained by studying the dependence of molecular weight and radius of gyration on elution volume. The calibration curves of molecular weight vs elution volume, for the polymer in the THF solutions, are also presented in Figure 2, whereas the corresponding logarithmic plot of the root-mean-squared radii of gyration vs elution volume is depicted in Figure 3. Although THF without salt produces a good separation of the sample, the addition of salts clearly improves the linearity of the molecular weight vs elution volume plots. The molecular weight calibration curves obtained in THF with different salts (NaCl or LiCl) are very similar; thus, neither the kind of cation nor the salt concentration has a marked effect on these results. When THF without salt is used as eluent, the molecular weights obtained in the region of low elution volumes (i.e., in the region of the shoulder noted above) are lower than those obtained when a salt is added.

The information provided by the radius of gyration calibration curves of PAMPST in THF and salts solutions in THF (Figure 3) is similar to what is obtained from molecular weight curves. The presence of salt improves the separation and increases the linearity of the plots, mainly in the region of low elution volumes. The accuracy of the radius of gyration obtained in the region of high elution volumes (>12 mL) is less than that of molecular weight since the size of the polymer should be larger than $\lambda/20$ in order to notice the angular dependence of scattered light.

The results obtained in DMF are depicted in Figures 4 and 5. Figure 4 depicts the RI signal and the calibration curves of molecular weight vs elution volume, whereas Figure 5 shows one of the MALS signals (at 90°) and the calibration curves of radius of gyration vs elution volume for PAMPST when DMF and 0.2 M LiCl solution in DMF are used as eluents. With the aim of facilitating the comparison, the chromatograms of the polymer in THF and 0.1 M LiCl in THF are included. When using DMF without salt as eluent, the peaks appear at very low elution volumes, and the chromatograms are not completely reproducible since they depend on the concentration of the sample. The molecular weight calibration curve (Figure 4) is

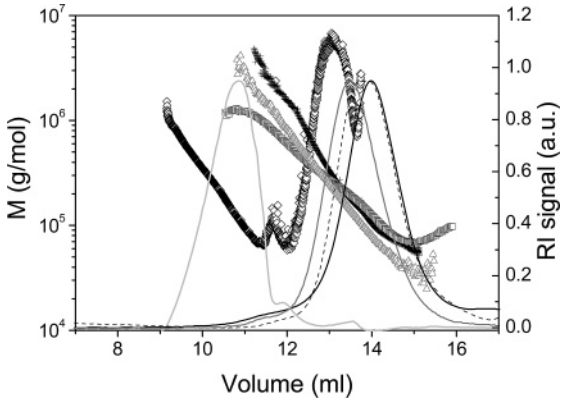

Figure 4. Molecular weight vs elution volume for PAMPST in different organic solutions: THF (square), DMF (diamond), THF/LiCl 0.1 M (triangle), DMF/LiCl 0.2 M (cross). Also depicted are the refractive index, RI, signals vs elution volume for PAMPST in THF as solid black line, DMF as light gray solid line, THF/LiCl 0.1 M as solid gray line, and DMF/LiCl 0.2 M as a black dash line.

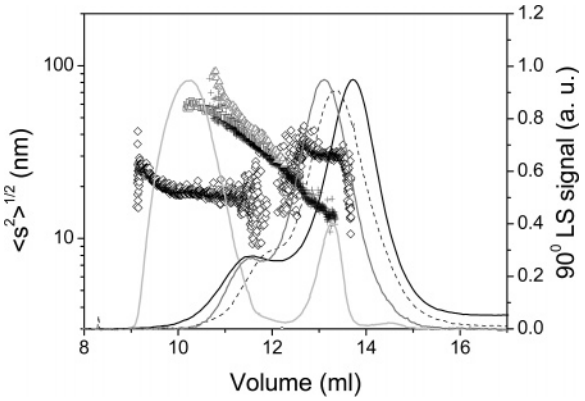

Figure 5. Radius of gyration and 90° MALS signal vs elution volume for PAMPST in the different solvents used. See legend for Figure 4.

linear in the first portion but presents upward curvature at higher elution volume. Moreover, the radius of gyration plot (Figure 5) shows a roughly constant value through the chromatogram, except for a small part at low elution volumes. All these results indicate that some other interactions mask the size exclusion separation mechanism. The addition of LiCl to the DMF noticeably improves the experimental results. Thus, the chromatograms are perfectly reproducible with different injections of the sample; the shape of the peaks and their elution volumes are closer to those obtained in THF. Furthermore, the molecular weight and radius of gyration plots (Figures 4 and 5) show a good separation in the same range as those obtained for the THF with salts. It is interesting to notice that the addition of salt improves the chromatogram in two eluents of very different polarity (i.e., values of the dielectric constant are $\epsilon = 36$ and 7.6 respectively for DMF and THF).

3.1.1. Differences between THF and DMF. The different behavior observed for the ionomer in the two eluents used could be explained on the basis of the polarity difference between THF and DMF. The Coulombic interaction between two ions of opposite charge is inversely proportional to the dielectric constant; thus, in THF ($\epsilon = 7.6$) the thermal energy at 25 °C is not enough to separate the ion pairs, while in DMF ($\epsilon = 37$) there is dissociation of some ionic moieties, giving a negative charged chain that behaves as a polyelectrolyte. These charges are responsible for the non-size-exclusion behavior of the polymer in DMF, as can be seen on the chromatograms and molecular weight and radius of gyration plots.

The different behavior observed for the polymer by SEC-MALS, in THF and DMF, is in very good agreement with the viscosity results obtained by Peiffer et al.[15] for a similar polymer, the sodium salt of the poly(2-acrylamido-2-methyl-1-propanesulfonic acid-*co*-styrene) with a 4.1 mol % of sulfonated groups, in THF and DMF solutions. The authors observed that this polymer did not show polyelectrolyte behavior in THF solution, and the results closely resemble those obtained for the unfunctionalized polystyrene. Moreover, the reduced viscosity of the polystyrene was somewhat lower than that of the sulfonated copolymer. On the contrary, the reduced viscosities of the copolymer in DMF were not only higher than those in THF at the same concentration, but they shown typical polyelectrolyte behavior as well. Thus, the reduced viscosity vs concentration plot exhibits an upward curvature at low polymer concentrations in DMF. The high dielectric constant of DMF favors higher levels of ionization of the sulfonated group, the ionic moieties attached to the chain repel, and the reduced viscosity increases with dilution for other ionomers. Similar viscosity behavior has been described for other ionomers.[11,20,21] Thus, the polyelectrolyte behavior of PAMS is also the reason for the abnormal chromatograms and the low elution volumes obtained in SEC with DMF as eluent (Figures 4 and 5).

3.1.2. Addition of Salt to THF. In low-polarity solvents such as THF the ion pairs form electric dipoles that can aggregate due to attractive forces, which must overcome the entropic and elastic forces exerted by the chain to which they are attached. These ion pair associations have been reported to be intra- or intermolecular depending on the ionomer concentrations.[20−23] The addition of low molecular weight electrolytes, such as NaCl or LiBr, to THF has a screening effect on the ion pair associations. Thus, the addition of salts to THF moves the chromatogram to lower elution volumes. More information can be obtained from the comparison of molecular weight and radius of gyration plots in THF and THF with salt. As can be seen in Figures 2 and 3, the range of molecular weights (and radius of gyration) is approximately the same in THF with and without salt, although curvatures appear in THF at low and high elution volumes, indicating that the size exclusion separation is worse in THF without salt.

3.1.3. Addition of Salt to DMF. As explained before, the addition of LiBr to DMF has a remarkable effect on the chromatograms, much more noticeable than in a less polar solvent such as THF (Figures 4 and 5). This is similar to the effect of salts on the solution properties of polyelectrolytes in water: The salt screens the electrical charges in the chain, and the ionomer behaves more like a neutral polymer.[11,21] It is interesting to note that the range of molecular weights and radius of gyration are similar in THF and DMF provided that salt has been added. Some additional information can be obtained from the scaling laws presented below.

3.2. Scaling Laws. The q parameter of the scaling law (eq 3) relating the size (radius of gyration) and the molecular weight provides information about the shape and size of the polymer and the thermodynamic quality of the solvent.[4,5] The scaling laws for the PAMPST in THF and 0.2 M LiCl solution in THF are presented in Figure 6. The scaling laws obtained for the other salt solutions in THF are similar and are not depicted. All the values of the q and Q parameters for the different eluents used are collected in Table 1. The addition of salt improves the linearity of the scaling law obtained in a wider range. Moreover, the value of $q \approx 0.65$ found for the polymer in THF diminishes with the addition of salt down to values of 0.6, corresponding to a random coil polymer in a good solvent. The effect of the addition of NaCl is somewhat smaller than LiCl since the NaCl solubility in THF is very low.

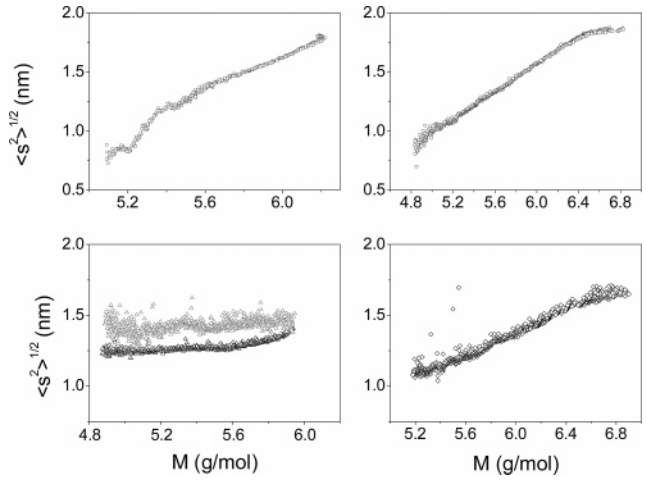

Figure 6. Scaling laws for PAMPST in different solvents: THF (square), DMF (triangle): results with eq 1 in black, with eq 4 in gray, THF/LiCl 0.2 M (circle), DMF/LiCl 0.2 M (diamond).

Table 1. Summary of Experimental Results Obtained by SEC-MALS for PAMPST Employing Different Eluents

eluent	10^3Q	q	$10^4\langle s^2\rangle_0/M$ (nm^2 mol g^{-1})	C_n
THF	5.0	0.65	7.0	10[a]
THF/LiCl 0.05 M	7.4	0.62	7.9	11
THF/LiCl 0.1 M	8.5	0.60	7.8	11
THF/LiCl 0.2 M	11.8	0.59	8.5	12
THF/$NaCl_{sat}$	5.2	0.64	7.8	11
DMF/LiCl 0.2 M	128	0.38	8.8	12

[a] Estimated error ca. 20% (see text).

The scaling law for DMF and the corresponding 0.2 M LiCl are also depicted in Figure 6. As pointed out above, the separation in DMF without salt is not efficient, and this fact is evident in the scaling plot which does not follow the power law. Thus, the curved scaling law obtained in DMF corroborates that this solvent is not suitable for a good size exclusion chromatographic separation as the logarithmic plots of molecular weight and radius of gyration (Figures 4 and 5) showed.

Since PAMPS behaves as a polyelectrolyte in pure DMF, the applicability of the light scattering equation (eq 1) can be questioned. We have tested a more general light scattering equation which takes into account the strong interactions among polymer chains and that has proved to be perfectly adequate for sulfonated polystyrene ionomers in salt-free DMF solutions.[24] This equation can be expressed in a simple form as

$$\frac{Kc}{\Delta R_\theta} = b_0 + b_1\left[\frac{4\pi}{\lambda}\sin\left(\frac{\theta}{2}\right)\right]^2 + b_2\left[\frac{4\pi}{\lambda}\sin\left(\frac{\theta}{2}\right)\right]^4 \qquad (4)$$

where the intercept $b_0 = Kc/\Delta R_0$ is the reciprocal of molecular weight for the low concentrations used in SEC-MALS, and the normalized slope b_1/b_0 is an apparent square radius of gyration since it includes the term on intermolecular interferences.[24] The true radius of gyration can be obtained from the slope at zero concentration.

$$\frac{b_1}{b_0} = \frac{\langle s^2\rangle_z}{3} - \frac{\xi^2}{6}\left(1 - \frac{\Delta R_0}{MKc}\right) \qquad (5)$$

The scaling law obtained, using eq 4 instead of eq 1, is depicted with gray triangles in Figure 6. As can be seen in the figure, the differences are larger for radius of gyration than for

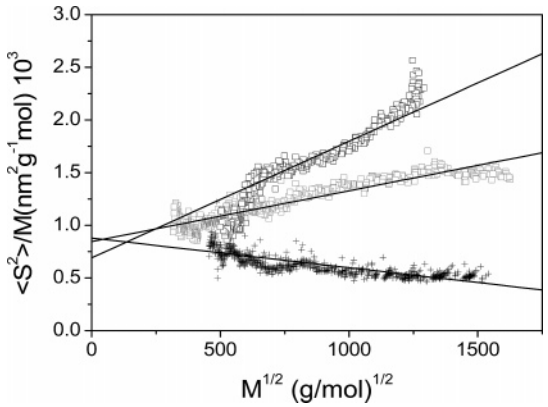

Figure 7. Fixman extrapolations to unperturbed dimensions for PAMPST in different solvents: THF (square), THF/LiCl 0.2 M (circle), DMF/LiCl 0.2 M (cross).

molecular weight. However, the scaling law clearly shows that the separation in the chromatographic column is not a simple size exclusion process, and therefore neither eq 1 nor eq 4 can be applied because the slices across the chromatogram are not monodisperse. Differences among the results obtained with eqs 1 and 4 for all other systems (i.e., pure THF and salts solutions in either DMF or THF) are negligible, and all the results shown for these systems were obtained with eq 1.

The addition of LiCl to DMF affords a suitable scaling law with a value of $q = 0.40$, which indicates that the polymer behaves as a random coil below theta conditions. DMF is worse solvent for polystyrene than THF,[18] and as stated above, the salt screens the charges in the ionomer. Thus, it is no surprising that THF is a good solvent, whereas DMF is a bad solvent for the ionomer.

3.3. Unperturbed Dimensions. The relationship between the dimensions of a polymer in a given solvent and the dimensions at unperturbed (i.e., theta) conditions is given by[14]

$$\langle s^2\rangle = \alpha^2\langle s^2\rangle_0 \tag{6}$$

where the expansion factor, α, depends on the quality of the solvent and the molecular weight of the polymer chain. The expansion factor becomes unity in two circumstances: first, at theta conditions when the dimension of the chain reaches the unperturbed value and, second, at the limit of such a low molecular weight that the interaction between segments of the same chain is not possible. Thus, unperturbed dimensions can be evaluated from measurements of dimensions of the polymers as a function of molecular weight in a good solvent, using several extrapolation procedures. When the SEC-MALS technique is applied to a broad polydisperse polymers, as in this case, a set of values of M and $\langle s^2\rangle$ is collected (see Figures 2−5) that can be used to evaluate unperturbed dimensions.[6,7] The Fixman extrapolation method[25] was used in the present work. The procedure is defined in eq 5 and provides $\langle s^2\rangle_0/M$ as the intercept:

$$\frac{\langle s^2\rangle}{M} = \frac{\langle s^2\rangle_0}{M} + 0.0299B\left(\frac{\langle s^2\rangle_0}{M}\right)^{-1/2} M^{1/2} \tag{7}$$

B represents the extent of the solvent−polymer interaction and can be related to Flory's interaction parameter, χ_1, through $B = \upsilon_p^2(1 - 2\chi_1)/V_{m,1}N_{Av}$, where υ_p is the specific volume of polymer and $V_{m,1}$ the solvent molar volume.

Fixman plots for PAMPST in THF, THF solutions (0.2 M LiCl), and DMF (0.2 M LiCl) are represented in Figure 7. All the plots for the polymer in the different THF salt solutions show a positive slope, and since they are similar to the one in 0.2 M LiCl are not depicted in the figure. The 0.2 M LiCl solution in DMF plot is different and exhibits a negative slope as a consequence of its below theta conditions. The values of the unperturbed dimensions $\langle s^2\rangle_0/M$, in nm^2 mol g^{-1}, obtained from the intercepts of the extrapolations in all the eluents used (except for DMF without salt, which is unsuitable as explained above), are collected in Table 1. It is noteworthy to remark that the extrapolations in THF and DMF with salt yield the same value of intercept in spite of the fact that THF is a good solvent, whereas DMF is a bad solvent for the polymer.

As explained before, the chromatographic separation for the salt-free PAMPS solution in THF is better than in DMF, but it still presents non-size-exclusion behavior that can be eliminated through addition of salt. Thus, although it is possible to perform a graphical extrapolation to unperturbed conditions that provides approximately the same intercept that is obtained in presence of salt, the accuracy of such an extrapolation is very poor. The quality of the extrapolation is improved by disregarding the data corresponding to very high and very low molecular weight (i.e., where the calibration curve presents noticeable curvature as can be seen in Figures 2 and 3). However, we estimate than even after disregarding these data, the error of the intercept is about 20%. All these difficulties can be surmounted through addition of the ionic salt.

The unperturbed dimensions of a polymeric chain are customarily represented by the characteristic ratio C_n, defined as the ratio of the unperturbed dimensions of the real chain to the dimensions of a freely jointed chain containing the same number of skeletal bonds. The characteristic ratio C_n can be calculated from the extrapolated values of $\langle s^2\rangle_0/M$ as[4]

$$C_n = \frac{\langle r^2\rangle_0}{nl^2} = \frac{6M_0}{2l^2}\frac{\langle s^2\rangle_0}{M} \tag{8}$$

where n is the number of skeletal bonds, each one of them having a length $l = 0.154$ nm in the present work, $\langle r^2\rangle_0$ the unperturbed value of the mean-square end-to-end distance, and M_0 the molecular weight of the repeating unit. The $\langle r^2\rangle_0 = 6\langle s^2\rangle_0$ relationship, valid for flexible chains, was used in the above equation. The values of C_n obtained are depicted in the last column of Table 1.

The unperturbed dimensions of polystyrene[18] correspond to $C_n \approx 10$ and do not depend on the solvent used for the extrapolations, as it is habitual in noncharged polymers. The ionomer studied in this work has 95 mol % styrene moieties, and its unperturbed dimensions obtained in salted THF or DMF are slightly larger, $C_n \approx 11-12$, indicating that, provided that a salt of low molecular weight is added to screen the ionic moieties, the unperturbed dimensions are close to those of polystyrene. However, when no salt is added, abnormal results can be found, especially in a polar solvent such as DMF.

3.4. Fluorescence Measurements. Excimer emission in solution of a polymer that contains chromophores along the chain can provide information about the shape and size as well as the possible aggregation processes in each particular solvent. An increase in intramolecular excimers is usually attributed to a more compact polymer conformation, in which chromophores placed far away along the chain come close together.[16,17] Nevertheless, intermolecular excimers, other form of excimer population, can supply information about the interchain interactions.

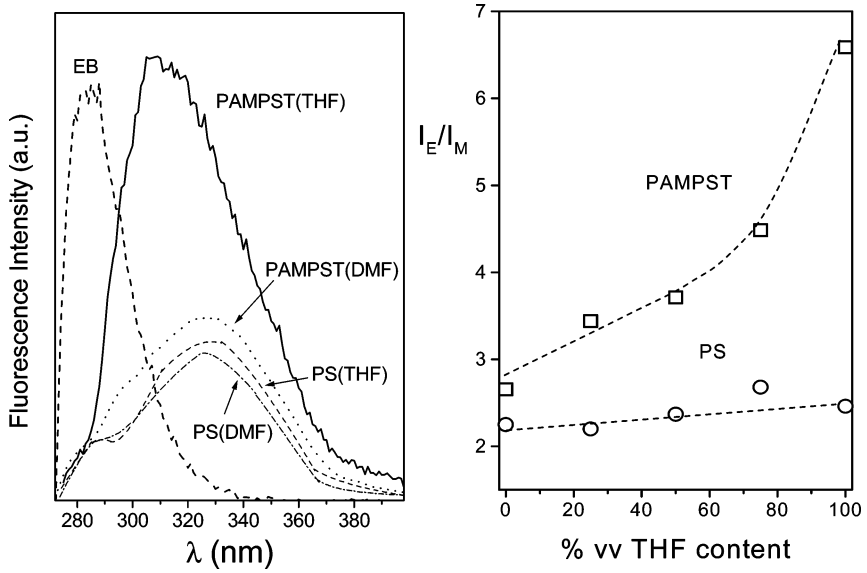

Figure 8. Left panel: uncorrected emission spectra for ethylbenzene (EB) in THF and PAMPST and PS in THF and DMF diluted solution at 25 °C upon 262 nm as excitation wavelength. Right panel: emission-to-monomer emission intensity ratios, I_E/I_M, for PAMPST and PS as a function of solvent THF:DMF composition measured as % vv THF content.

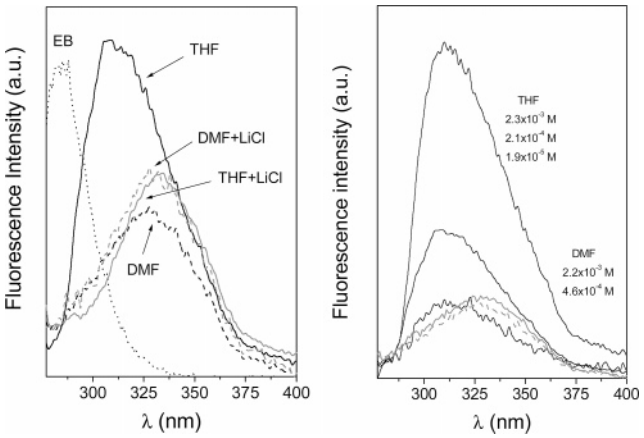

Figure 9. Left panel: uncorrected emission spectra for ethylbenzene (EB) and PAMPST in THF and DMF pure solvents and in the presence of LiCl salt at 25 °C upon $\lambda_{exc} = 262$ nm. The concentrations used were in the 10^{-4} M magnitude order, similar to the ones in SEC measurements. Right panel: uncorrected emission spectra for PAMPST in THF (black) and DMF (gray) at different concentrations.

The left panel of Figure 8 depicts the normalized (at ~285 nm) emission spectra for PAMPST and PS standard in dilute solution of THF and DMF and the ethylbenzene model compound in THF upon excitation of benzene groups (absorbance <0.4 at $\lambda_{exc} = 262$ nm). As expected, the model compound exhibits a single monomer band, whereas polymers show a broadening of the emission to the red due to the excimer formation between benzene groups of PS residues. The amount of this band seems to depend on the polymer and the nature of the solvent. The right panel of Figure 8 shows the dependence of the excimer-to-monomer ratios I_E/I_M on the solvent DMF/THF composition for dilute solution of both polymers. Against expectation, the excimer-to-monomer ratio I_E/I_M is almost independent of the solvent composition for PS despite that DMF is a worse solvent for PS than THF. Moreover, the presence of a few units containing the $SO_3^-H^+$ moiety in a PS chain, e.g., PAMPST, makes the I_E/I_M ratios increase substantially with the content of THF in the solvent mixture.

As depicted in the left panel of Figure 9, LiCl salt addition does not seem to modify the size of the excimer band of the PAMPST/DMF solutions. However, it drastically decreases when the solvent used is THF despite the fact that the THF solvent quality seems to decrease slightly in the presence of LiCl salt. Excimer emission also strongly depends on the PAMPST concentration in THF, and it hardly occurs for any of the PAMPST−THF + LiCl, PAMPST−DMF, and PAMPST−DMF + LiCl polymer systems, as shown in the right panel of Figure 9. These results indicate that intramolecular excimer does not seem to be very sensitive to the polymer solvent quality for any of the solvents used. However, they also infer that interchain interactions are responsible for the large population of excimers in the PAMPST/THF system that does not take place in other solvents used in our measurements.

4. Theoretical Calculations

4.1. Molecular Dynamics Software and Procedures. The Amber molecular modeling package,[26] including the Amber force field, was employed for all the molecular dynamics (MD) simulations presented below. Coulombic potentials were computed by the Ewald sum procedure.[26] Partial charges were assigned to every atom by means of the MOPAC package and the AM1 procedure.[27] A time step $\delta = 1$ fs (i.e., 1×10^{-15} s) was employed for the integration algorithm. Bonds involving H atoms were kept at fixed length by means of the SHAKE algoritm.[28]

The compositions of the systems studied are summarized in Table 2. The basic molecule is an oligomer containing 84 repeating units whose structure is schematically represented in Figure 1. Four of these units (i.e., 5 mol %) contain the amide residue (AM) as side groups while all the other contain a phenyl group (i.e., they are regular polystyrene units). The chain contains 50% meso units with random placement of meso and racemic diads. Three of these oligomers were packed into a cubic box having periodic boundary conditions together with 750 molecules of solvent (either THF or DMF) and, in some of the systems, 100 molecules of a ionic salt (either NaCl or LiCl). The side length of the periodic boundary conditions boxes were adjusted as to reproduce macroscopic densities of THF and DMF solvents (ca. $\rho \approx 0.89$ and 0.84 g cm^{-3} respectively for THF and DMF). All the MD simulations were performed under NVT conditions with the temperature being kept constant

Table 2. Composition of the Systems Studied in the Present Work[a]

		solvent		ions			
system	model molecules	THF	DMF	Cl^-	Na^+	Li^+	L (Å)
OT-1	3	750					53.42
OT-2	3	750		100	100		54.66
OT-3	3	750		100		100	54.33
OD-1	3		750				51.62
OD-2	3		750	100	100		53.73
OD-3	3		750	100		100	53.40

[a] The structure of the oligomer is schematically represented in Figure 1. The side length of the periodic boundary conditions box is adjusted as to reproduce macroscopic densities of THF and DMF solvents (ca. $\rho \approx 0.89$ and 0.84 g cm^{-3} respectively for THF and DMF).

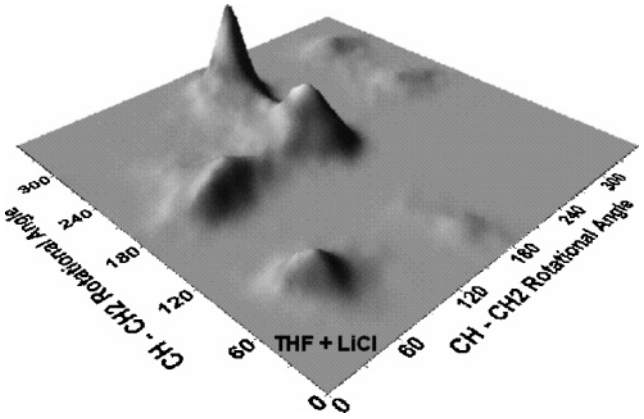

Figure 10. Distribution of conditional probabilities for the pair of skeletal bonds $CH_2-CH-CH_2$ flanking an AM group (i.e., central pair of bonds in Figure 1) in a meso−racemic triad of system OT-3 (i.e., oligomers, THF, and LiCl).

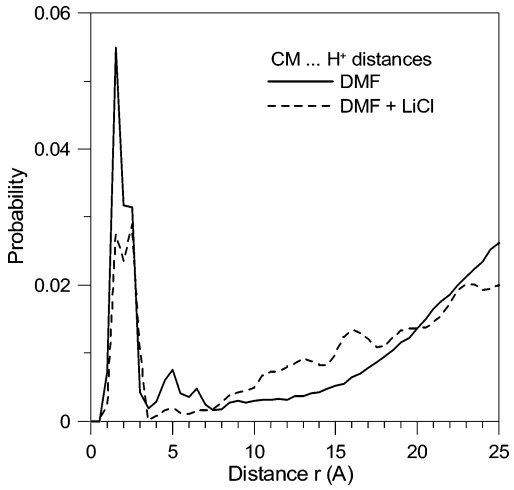

Figure 11. Probability of finding the center of masses of the three O of any SO_3^- group (CM) separated a distance r from a H^+ ion obtained from MD trajectories performed on systems OD-1 (pure DMF as solvent) and OD-3 (DMF + LiCl as solvent). See text for details.

by means of the Berensen[28] thermostat with a coupling factor of 1000 fs. Several exploratory calculations were performed at different temperatures ranging from 300 to 700 K. Finally, it was decided to perform all the calculations at 700 K in order to increase the atomic velocities,[29] thus facilitating the passage over energetic barriers and consequently improving the sampling of all the configurational space.

Each system was initially built within a rather large box having approximately twice the final side length. The size of these initial boxes was progressively decreased by a combination of MD and energy minimization steps. More specifically, the actions taken were as follows: After each decrease of the side box, a 60 ps (i.e., 60×10^{-12} s) MD simulation was performed, during which the system was slowly warmed up from 0 to 700 K, equilibrated at this temperature for ~20 ps, and then slowly cooled down to 0 K. Then, the energy of the system was minimized with respect to all internal coordinates with a combination of steepest descendent and conjugated gradient algorithms.[26] Once the system has reached the desired volume, it was slowly warmed up from 0 to 700 K, employing 100 ps in this process. Finally, the production stage was started which consisted of 4×10^6 integration cycles (i.e., a time span of 4000 ps), during which the coordinates of the system were recorded at intervals of 1 ps, thus producing a total of 4000 snapshots of the system that was employed in the posterior analysis. Results obtained during the warming step were not employed in the analysis.

4.2. Distribution of Rotational Isomers. No noticeable difference on the distribution of rotational angles over the skeletal bonds was found among the systems studied. Thus, Figure 10 shows the distribution of conditional probabilities for the pair of bonds $CH_2-CH-CH_2$ flanking an AM group in a meso−racemic triad of system OT-3 (i.e., oligomers, THF, and LiCl). It shows a strong preference for the gt conformation followed by tt. The results are very similar for all the other systems, and in fact, they are not too different from what is found for a similar pair of bonds in a polystyrene chain.

Consequently, the differences in experimental behavior observed among these systems cannot be attributed to large differences in the distribution of rotational angles over the skeletal bonds. On the contrary, they should be produced by long-range interactions either intra- or intermolecular. Furthermore, when the long-range interactions are canceled through extrapolation to unperturbed conditions, all the systems should produce roughly the same unperturbed dimensions which should not be too different from those of polystyrene.

4.3. Distribution of Interatomic Distances. All the systems contain 12 SO_3^- groups and 12 H^+ ions. Each SO_3^- group was represented by the position of the center of masses of the three O atoms which will be designated as CM hereafter. The distances from each CM to other pertinent items of the system (i.e., other CM, H^+, Cl^-, Na^+, and Li^+ ions) were computed for each conformation recorded along the MD trajectories of each system. The results obtained with NaCl salt are almost undistinguishable from those of LiCl salt. So it seems that the behavior of the system is not sensitive to the nature of the cation contained in the ionic salt. Only the results obtained with LiCl will be shown hereafter.

The distribution of distances between CM and H^+ ions is shown in Figures 11−13. Figures 11 and 12 represent the differential distributions and were obtained by counting how many times any of the CM...H^+ distances along the MD trajectory lied within the interval $r \pm \delta r$ with $\delta r = 0.25$ Å. Thus, for instance, the values indicated for $r = 5$ Å represent the fraction of CM...H^+ distances comprised between 4.75 and 5.25 Å. These results are paramount to the unnormalized $g(r)$

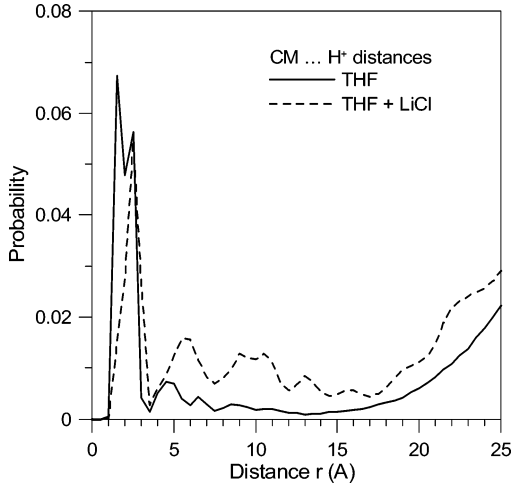

Figure 12. Same as Figure 11 for systems OT-1 (pure THF) and OT-3 (THF + LiCl).

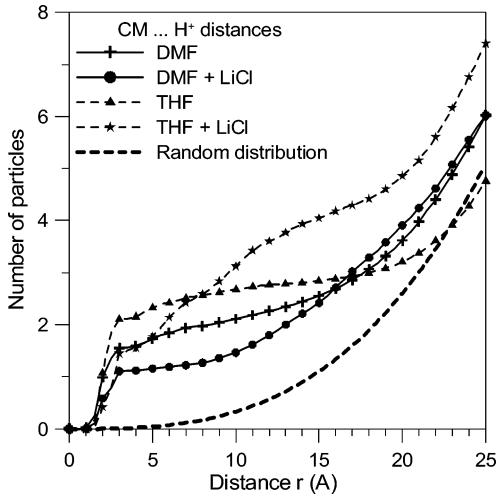

Figure 13. Number of H^+ ions that can be found at a distance equal to or smaller than r from a CM. Results were obtained from MD trajectories of systems OD-1, OD-3, OT-1, and OT-3. Thicker broken line represents the values that would be obtained with a random distribution of CM and H^+.

pair distribution function.[30] Figure 13 represents the number of particles n placed within a distance smaller than or equal to a given value of r. It was computed by counting how many times a CM...H^+ distance lied within the interval $0-r$ and multiplying this fraction by the total number N of H^+ particles contained in the system. The thick broken line in Figure 13 represents the distribution obtained by assuming that all the particles were randomly distributed within the system. In such case, the number n of H^+ ions placed within a distance r of any given CM would be proportional to the volume of a sphere of radius r, i.e., $n = N(r/R)^3$, with R being the radius of an sphere having the same volume of the periodical box containing the system. In fact, this line should be different for each one of the systems represented in Figure 13 because the boxes containing those systems have different side lengths (see Table 2). However, the differences are too small as to be of any significance, and the line shown in Figure 13 was computed with the average of the side lengths indicated in Table 2.

According to Figures 11 and 12, there is a strong probability of finding a CM...H^+ distance of ca. 2.5 Å in all the systems, but in the case of THF a second peak appear at a slightly higher value of r, i.e., $r \approx 3$ Å. The distribution of particles is best seen in Figure 13, which clearly indicates that the number of

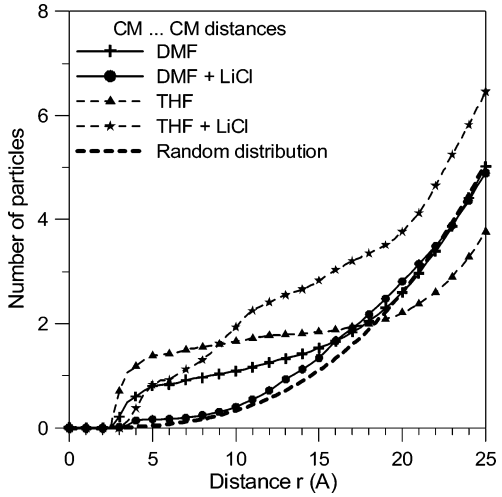

Figure 14. Same as Figure 13 from CM...CM distances.

particles surrounding any given one is always much larger than what would be obtained with a random distribution up to distances of ca. 22−25 Å. The fist neighbor (i.e., $n = 1$) is located at a distance of ca. 2.5 Å in all the systems. This distance is larger than what corresponds to a O−H chemical bond and indicates that the $SO_3^-H^+$ groups is dissociate although it remains as an ionic pair at a relatively short distance. Only in the case of pure THF is a second H^+ located at ca. 3 Å. In the case of DMF, the second H^+ is placed at distances larger than 10 Å. Addition of LiCl increases the distance to the second neighbor in both cases, with the effect being stronger in the case of DMF than in THF.

The distribution of CM...CM distances is not shown because it is very similar to the distribution of CM...H^+ distances (Figures 11 and 12) with the only noteworthy difference than the peaks of maximum probability appear at distances that are roughly 1 Å larger in the former case; i.e., CM are more separated among themselves than with their respective H^+ counterions The number n of CM that can be found at a given distance of other CM is represented in Figure 14, which is the equivalent to Figure 13 for CM...H^+. According to Figure 14, pure THF exhibits a behavior which is noticeably different from all the other systems and also very different from a random distribution. Thus, in the case of THF, each CM has a second CM ($n = 1$ in Figure 14), at a distance of ca. 3.5 Å, but the next one is placed at about 16 Å. In the case of DMF, the first neighbor is placed at ca. 8 Å and the second one at ca. 16 Å. As in the case of CM...H^+, addition of the ionic salt increases the separation from CM to first and second CM neighbors, with the effect being stronger in the case of DMF. In fact, according to Figure 14, the system oligomers + DMF + LiCl contains a nearly random distribution of CM...CM distances.

Finally, Figure 15 indicates that the distribution of CM...Cl^- and CM...Li^+ distances are similar in both solvents and very different from what would be obtained by a random distribution. It is interesting to point out that the first Li^+ ion is placed at a distance which is roughly 1 Å smaller than that of the first Cl^- ion. This is a straight consequence of the neat negative charge of the SO_3^- group.

This behavior can be summarized very easily: Electrostatic interactions are strong enough as to keep $SO_3^-H^+$ groups forming ionic pairs in all the systems, but these groups will aggregate in pairs only in the case of pure THF. In this case, the $SO_3^-H^+$ groups will tend to aggregate in pairs (each CM has a second CM close to it), sharing their respective H^+ ions at distances in which the sum of electrostatic interactions among

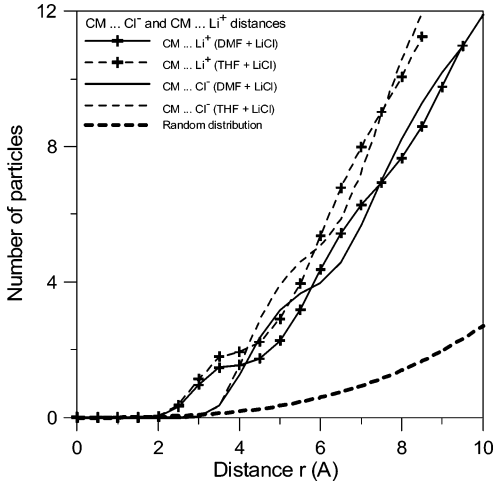

Figure 15. Number of Cl^- and Li^+ ions that can be found at a distance equal to or smaller than r from a CM. Results were obtained from MD trajectories of systems OD-3 and OT-3. Thicker broken line represents the values that would be obtained with a random distribution of particles.

all the charged particles results attractive. However, it is enough to add some ionic salt or to increase the dielectric constant of the system for preventing the formation of aggregates. When an aggregate of two SO_3^- groups is formed, the phenyl rings of the styrene groups flanking one of the amide residues are placed relatively close to the phenyl rings flanking the second amide residue, so that they can adopt the planar sandwich arrangement that produces excimer fluorescence emission. According to the theoretical results, this emission will be much stronger in pure THF solvent than in any of the other three systems, which is in good agreement with the fluorescence measurement. Furthermore, the fact that the experimental excimer emission in THF solution increases with the polymer concentration indicates that these kinds of aggregates are intermolecular.

4.4. Chain Dimensions. Mean-squared distances $\langle r^2\rangle$ between skeletal C atoms separated by $x = 41$, 62, and 84 repeat units were computed. The slope of a $\log(\langle r^2\rangle^{1/2})$ vs $\log(x)$ plot gives the q parameter of the scaling law (eq 3) provided that the chain is long and flexible enough as to fulfill the relationship $\langle r^2\rangle \approx 6\langle s^2\rangle$, and for this reason we have not calculated $\langle r^2\rangle$ for smaller chains. It should be pointed out that MD simulation is not a good procedure for calculating chain dimensions in relatively long chains because the number of allowed conformations (ca. $3^{166} \approx 10^{79}$ for $x = 84$ in this work) is far too huge as to allow a good statistical sampling even at the high temperature employed in the present calculation. For this reason, the correlation among the data obtained is rather poor. But, at any rate, the results indicate that $\langle r^2\rangle^{1/2}$ increases much faster with x in the cases of THF and THF + LiCl than in DMF or DMF + LiCl. In fact, the q parameter is roughly 0.6 in THF or THF + LiCl, indicating that these are good solvents for this polymer. On the contrary, $q \approx 0.4$ is obtained for both DMF and DMF + LiCl solvents, indicating that these systems are below unperturbed conditions. These results are in good agreement with the experimental values obtained by SEC and are a straight consequence of the fact that 95% of the repeat units of PAMPST are styrene units, and THF is a much better solvent than DMF for polystyrene.

5. Conclusions

THF and the different salt solutions in THF are very good solvents for PAMPST, whereas DMF with salt is a poor solvent for the polymer. Data of radius of gyration vs molecular weight, in salted THF or DMF, provide very good fittings to scaling laws with values of the q exponent 0.6 in the case of THF solution and 0.4 in the case of DMF solution. In spite of the different thermodynamic quality of the solvents, similar extrapolations to unperturbed conditions are obtained in the case of THF and DMF salt solutions and, although with bigger error, for pure THF. Thus, all the extrapolations give roughly the same value of $\langle s^2\rangle_0/M$, providing a characteristic ratio of ca. $C_n \approx 11-12$.

Results of theoretical calculations support the experimental findings. Thus, they suggest that unperturbed dimensions of the polymer chain should be roughly the same in all the systems studied here. The $SO_3^-H^+$ groups aggregate into pairs in the case of THF solvent. Such aggregates are formed in none of the other solvents (i.e., DMF, DMF + LICl or THF + LiCl). The structure of these aggregates explains why the fluorescence excimer emission is much stronger in pure THF than in all other systems, and furthermore, it increases with increasing concentration of polymer. Finally, the variation of $\langle r^2\rangle$ with the number of repeat units x suggests that the systems are above (below) unperturbed conditions in THF (DMF) solutions.

Acknowledgment. This research was supported by Comunidad de Madrid (CAM projects: GR/MAT/0810/2004; S-055/MAT/0227), CICYT (project CTQ2005-04710/BQU), and the grant PFPU (G.M.).

References and Notes

(1) Potschka, M.; Dubin, P. L. *Strategies in Size Exclusion Chromatography*; American Chemical Society: Washington, DC, 1996.
(2) Wyatt, P. J. *Anal. Chim. Acta* **1993**, *271*, 1.
(3) Laguna, M. T. R.; Medrano, R.; Plana, M. P.; Tarazona, M. P. *J. Chromatogr. A* **2001**, *13*, 919.
(4) Flory, P. J. *Statistical Mechanics of Chain Molecules*; Wiley: New York, 1969.
(5) De Gennes, P. G. *Scaling Concepts in Polymer Physics*; Cornell University Press: Ithaca, NY, 1979.
(6) Tarazona, M. P.; Saiz, E. J. *Biochem. Biophys. Methods* **2003**, *56*, 95.
(7) Búrdalo, J.; Medrano, R.; Saiz, E.; Tarazona, M. P. *Polymer* **2000**, *41* 1615.
(8) Marcelo, G.; Saiz, E.; Tarazona, M. P. *Biophys. Chem.* **2005**, *113*, 201.
(9) Marcelo, G.; Tarazona, M. P.; Saiz, E. *Polymer* **2005**, *46*, 2584.
(10) Lundberg, R. D. *J. Polym. Sci., Polym. Phys.* **1982**, *20*, 1143.
(11) Hara, M. *Physical Chemistry of Polyelectrolytes*; Radeva, T., Ed.; Marcel Dekker: New York, 2001; Chapter 9.
(12) Nomula, S.; Cooper, S. L. *Macromolecules* **2001**, *34*, 925.
(13) Neilson, R. H.; Hani, R.; Wisian-Neilson, P.; Meister, J. S.; Roy, A.; Hagnauer, G. L. *Macromolecules* **1987**, *20*, 910.
(14) Gleria, M.; De Jaeger, R. *Phosphazenes: a Worldwide Insight*; Nova Science Publishers: Hauppauge: NY, 2002.
(15) Peiffer, D. G.; Kim, M. W.; Kaladas, J. J. *Polymer* **1988**, *29*, 716.
(16) Guillet, J. *Polymer Photophysics and Photochemistry: An Introduction to the Study of Photoprocesses in Macromolecules*; Cambridge University Press: New York, 1985; Chapter 7.
(17) Rabeck, J. F. *Mechanism of Photophysical Processes and Photochemical Reactions in Polymers*; John Wiley and Sons: New York, 1987.
(18) Brandrup, J.; Immergut, E. H.; Grulke, E. A. *Polymer Handbook*, 4th ed.; John Wiley: New York, 1999.
(19) Huglin, M. B. *Light Scattering from Polymer Solutions*; Academic: London, 1972.
(20) Campos, A.; Garcia Suñer, R I.; Figueruelo, J. E. *Polymer* **1997**, *38*, 3011.
(21) Hara, M.; Wu, J.; Lee, A. H. *Macromolecules* **1989**, *22*, 754.
(22) Eisenberg, A.; Hird, B.; Moore, B. R. *Macromolecules* **1990**, *23*, 4098.
(23) Young, A. M.; Higgins, J. S.; Peiffer, D. G.; Rennie, A. R. *Polymer* **1996**, *37*, 2125.
(24) Bodycomb, J.; Hara, M. *Macromolecules* **1994**, *27*, 7369.
(25) Fixman, M. *J. Chem. Phys.* **1955**, *23*, 1656.
(26) http://www.amber.ucsf.edu/amber/amber.html.; http://www.amber.ucsf.edu/amber/dbase.html.; http://pharmacy.man.ac.uk/amber/.
(27) MOPAC, Quantum Chemistry Program Exchange (Department of Chemistry, Indiana University, Bloomington, IN).

(28) Allen, M. P.; Tildesley, D. J. *Computer Simulation of Liquids;* Clarendon: Oxford, 1987.

(29) Since *N*, *T*, *V* are kept constant, the systems are supposed to maintain a constant density (typical of ca. 300 K) even when the atoms are forced to move with velocities distributions typical of ca. 700 K. This is a rather crude approximation, but it is dictated by limitations in the computer power. If the simulations were run at ca. 300 K, the atoms will move rather slowly, so that a good statistical sampling of the conformational space would require unreasonably long CPU times.

(30) Our systems are contained in cubes of side, *L*. Thus, it seems reasonable to analyze the particles distribution on the basis of a spherical function that depends only on the distance *r* between particles up to $r = L/2$, which is more than enough for our purposes. However, the cube has a noticeable amount of volume at $r > L/2$ which contain a certain number of particles (different in each snapshot). Under these circumstances, we think that the normalization of the function might be questionable and preferred to use the unnormalized values.

MA0623845